Non-Fermi liquid behavior at flat hot spots from quantum critical fluctuations at the onset of charge- or spin-density wave order

Lukas Debbeler and Walter Metzner ⓘ

Max Planck Institute for Solid State Research, D-70569 Stuttgart, Germany

We analyze quantum fluctuation effects at the onset of charge- or spin-density wave order with a $2k_F$ wave vector $\mathbf{Q}$ in two-dimensional metals, for the special case where $\mathbf{Q}$ connects a pair of hot spots situated at high symmetry points of the Fermi surface with a vanishing Fermi surface curvature. We compute the order parameter susceptibility and the fermion self-energy in one-loop approximation. The susceptibility has a pronounced peak at $\mathbf{Q}$, and the self-energy displays non-Fermi liquid behavior at the hot spots, with a linear frequency dependence of its imaginary part. The real part of the one-loop self-energy exhibits logarithmic divergencies with universal prefactors as a function of both frequency and momentum, which may be interpreted as perturbative signatures of power laws with universal anomalous dimensions. As a result, one obtains a non-Fermi liquid metal with a vanishing quasiparticle weight at the hot spots, and a renormalized dispersion relation with anomalous algebraic momentum dependencies near the hot spots.

I. INTRODUCTION

Quantum fluctuations at and near quantum critical points (QCP) in metallic electron systems naturally lead to non-Fermi liquid behavior with unconventional temperature, momentum, and frequency dependencies of physical observables [1]. The fluctuation effects are most pronounced in low-dimensional systems. In view of non-Fermi or "strange metal" behavior observed in various layered compounds, such as the high-T_c cuprates, two-dimensional systems have attracted particular interest. Due to the complex interplay of critical order parameter fluctuations with gapless electronic excitations, the theory of such systems is notoriously difficult.

Metals at the onset of charge- or spin-density wave order provide a vast playground of quantum critical non-Fermi liquids with many distinct universality classes. The most intensively studied case of a Néel antiferromagnet is just one example [2–5]. A particularly intriguing situation arises when the wave vector $\mathbf{Q}$ of the density wave is a *nesting vector* of the Fermi surface, that is, when it connects Fermi points with collinear Fermi velocities [6]. Charge and spin susceptibilities exhibit a singularity at such wave vectors due to an enhanced phase space for low-energy particle-hole excitations. Since the nesting vectors in continuum systems are related to the Fermi momentum k_F by the simple relation $|\mathbf{Q}| = 2k_F$, one may refer to such nesting vectors also as "$2k_F$" vectors [7]. The wave vector (π, π) of a Néel state (in two dimensions) is a nesting vector only for special electron densities. Quantum

critical fluctuations lead to an enhanced quasiparticle decay rate in this case [8,9], but the decay rate remains parametrically smaller than the excitation energy of the quasiparticles in the low-energy limit [10].

Recently, non-Fermi liquid behavior at the onset of charge- or spin-density wave order with *incommensurate* [11] nesting wave vectors $\mathbf{Q}$ in two-dimensional metals has been analyzed in a series of papers. In a one-loop calculation of the fermionic self-energy, a breakdown of Fermi liquid behavior was obtained at the *hot spots* on the Fermi surface connected by the ordering wave vector [12]. If the ordering wave vector $\mathbf{Q}$ connects only a single pair of hot spots, in axial or diagonal direction, the frequency dependence of the one-loop self-energy at the hot spots obeys a power law with exponent $\frac{2}{3}$. If $\mathbf{Q}$ connects two pairs of hot spots, the imaginary part of the real frequency one-loop self-energy exhibits a linear frequency dependence. In none of these two cases the perturbative solution is self-consistent, and the feedback of the non-Fermi liquid self-energy seems to push the ordering wave vector away from the nesting point [13,14]. Actually it was argued already long ago, for the case of a single hot spot pair, that quantum fluctuations spoil the QCP in favor of a first-order transition [7]. However, a flattening of the Fermi surface at the hot spots might save the QCP [13], and this scenario was supported by a systematic ϵ expansion around the critical dimension $d_c = \frac{5}{2}$ [15]. For the two-hot-spot pair case, a self-consistent solution with a stable QCP was found numerically [14]. While fluctuations are naturally stronger in two-dimensional systems, quantum fluctuation effects at the onset of density wave order with a $2k_F$ wave vector are special and intriguing also in three dimensions [16]. In this paper we analyze quantum fluctuations and non-Fermi liquid behavior at the onset of density wave order in a two-dimensional system for a case where the nesting vector connects *flat* hot spots on a mirror symmetry axis, where the Fermi surface curvature
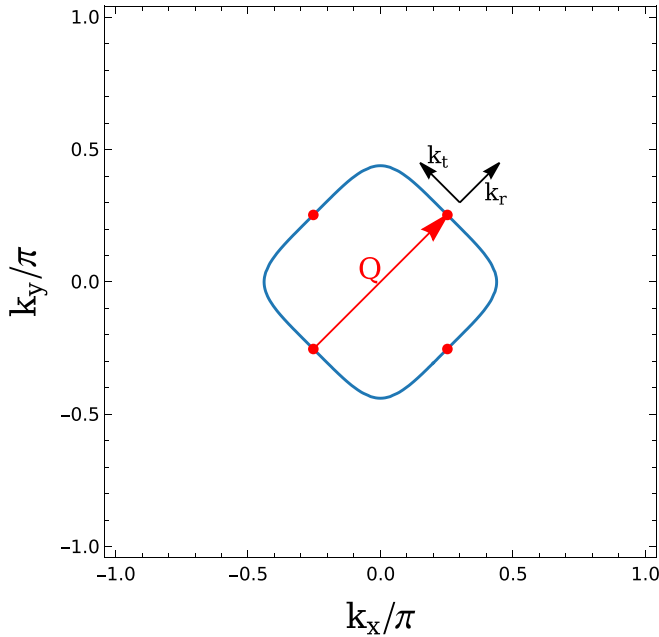
FIG. 1. Hot spots with vanishing curvature on the Fermi surface for a tight-binding model with nearest and next-nearest neighbor hopping amplitudes t and t', respectively, on a square lattice. The ratio of hopping amplitudes has been chosen as $t'/t = -0.35$, and the Fermi level leading to flat hot spots is $\epsilon_F = 8t'[1 - 2(t'/t)^2] = -2.114t$.

vanishes already in the noninteracting reference system, that is, before fluctuations are taken into account. Such a situation may arise at special electron filling factors. For example, for a tight-binding model with nearest and next-nearest neighbor hopping on a square lattice, the Fermi surface exhibits zero curvature points along the Brillouin zone diagonal for a specific choice of the Fermi level (corresponding to a special filling factor), as illustrated in Fig. 1. Using relative momentum coordinates k_r and k_t in normal and tangential directions, respectively, with respect to the Fermi surface at a hot spot, the dispersion relation near the hot spot has the form,

$$\xi_{\mathbf{k}} = \epsilon_{\mathbf{k}} - \epsilon_F = v_F k_r + b k_t^4, \qquad (1)$$

to leading order in k_r and k_t. Here v_F is the Fermi velocity at the hot spot, and b is a real constant, which is positive (negative) if the Fermi surface is convex (concave) at the hot spot. Due to the mirror symmetry with respect to the Brillouin zone diagonal there is no term of order k_t^3. Hence, this case differs from inflection points on the Fermi surface, where the curvature vanishes, too, but the leading tangential momentum dependence is of cubic order.

As in the above-mentioned case of Néel order with nested hot spots, a QCP with flat hot spots connected by an incommensurate wave vector requires tuning to a specific particle density. In addition, another parameter must be tuned such that the system is situated at the onset of charge- or spin-density wave order. In solids, the density of electrons in layered compounds can be varied over a broad range by chemical substitution or gate potentials. The tuning of other parameters such as the ratio of Coulomb to kinetic energy is in principle possible by pressure, but in practice limited to a

narrow regime. Alternatively, a QCP with flat hot spots may be realized by cold fermionic atoms in optical lattices, where the particle density, interaction strength, and hopping amplitudes can be tuned at will [17,18].

We compute the order parameter susceptibility, the effective interaction, and the fermion self-energy at the onset of incommensurate charge- or spin-density wave order with flat nested hot spots in a one-loop approximation. The susceptibility and the effective interaction exhibit pronounced peaks at the nesting vector. Both the momentum and frequency dependencies of the self-energy develop logarithmic divergencies, signaling a vanishing quasiparticle weight and non-Fermi liquid power laws with universal critical exponents.

The remainder of the paper is structured as follows. In Sec. II we compute the order parameter susceptibility and the effective interaction at the QCP. The momentum and frequency dependence of the fermion self-energy is evaluated in Sec. III. A conclusion in Sec. IV closes the presentation.

II. SUSCEPTIBILITY AND EFFECTIVE INTERACTION

We consider a one-band system of interacting fermions with a bare single-particle energy-momentum relation $\epsilon_{\mathbf{k}}$. We are dealing exclusively with ground-state properties, that is, the temperature is fixed to $T = 0$. The bare fermion propagator has the form,

$$G_0(\mathbf{k}, ik_0) = \frac{1}{ik_0 - \xi_{\mathbf{k}}}, \qquad (2)$$

where k_0 denotes the (continuous) imaginary frequency, and $\xi_{\mathbf{k}} = \epsilon_{\mathbf{k}} - \mu$. At zero temperature, the chemical potential μ is equal to the Fermi level ϵ_F. We assume that, in mean-field theory, the system undergoes a charge- or spin-density wave transition with an incommensurate and nested wave vector $\mathbf{Q}$, which connects a pair of hot spots on the Fermi surface. We further assume that the dispersion relation in the vicinity of the hot spots has a quartic tangential momentum dependence of the form Eq. (1).

In random phase approximation (RPA, that is, at one-loop level), the order parameter susceptibility has the form,

$$\chi(\mathbf{q}, iq_0) = \frac{\chi_0(\mathbf{q}, iq_0)}{1 + g\chi_0(\mathbf{q}, iq_0)}, \qquad (3)$$

where $g < 0$ is the coupling constant parametrizing the interaction in the instability channel. The bare charge or spin susceptibility χ_0 is related to the particle-hole bubble Π_0 by $\chi_0(\mathbf{q}, iq_0) = -N\Pi_0(\mathbf{q}, iq_0)$, where N is the spin multiplicity, and [19]

$$\Pi_0(\mathbf{q}, iq_0) = \int_{\mathbf{k}} \int_{k_0} G_0(\mathbf{k}, ik_0) G_0(\mathbf{k} - \mathbf{q}, ik_0 - iq_0). \qquad (4)$$

Here and in the following $\int_{\mathbf{k}}$ is a shorthand notation for $\int \frac{d^2\mathbf{k}}{(2\pi)^2}$, and $\int_{k_0}$ for $\int \frac{dk_0}{2\pi}$. While keeping the spin multiplicity N as a general parameter in our equations, we choose $N = 2$, corresponding to spin-$\frac{1}{2}$ fermions, in all numerical results. Continuing $\Pi_0(\mathbf{q}, iq_0)$ analytically to the real frequency axis from the upper complex frequency half-plane yields the retarded polarization function $\Pi_0(\mathbf{q}, \omega)$. In Fig. 2 we show the static (zero frequency) bare susceptibility $\chi_0(\mathbf{q}, 0) = -2\Pi_0(\mathbf{q}, 0)$ for a tight-binding model with parameters as in
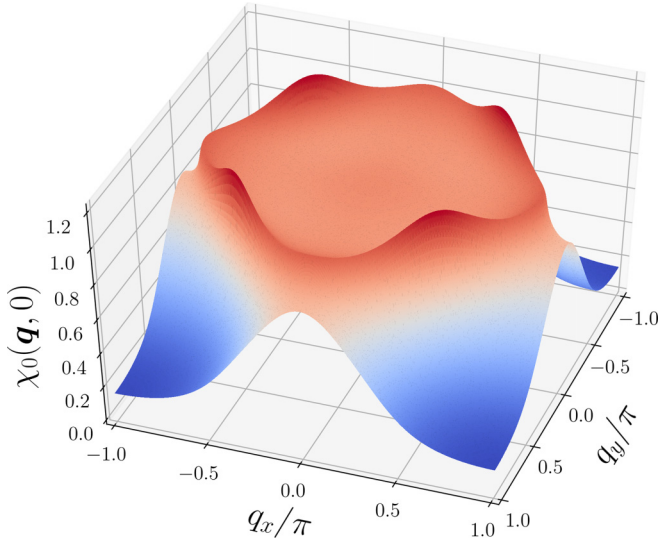
FIG. 2. Static bare susceptibility $\chi_0(\mathbf{q}, 0)$ as a function of $\mathbf{q}$ for a tight-binding model of spin-$\frac{1}{2}$ fermions ($N = 2$) with parameters as in Fig. 1.

Fig. 1 [20]. Pronounced peaks are visible at the nesting vectors connecting the four flat hot spots on the Fermi surface.

The RPA susceptibility diverges when $g\chi_0(\mathbf{Q}, 0) = -1$, signaling an instability at the critical coupling $g_c = -1/\chi_0(\mathbf{Q}, 0)$ toward charge- or spin-density wave order with one of the nesting wave vectors $\mathbf{Q}$ at which $\chi_0(\mathbf{q}, 0)$ has a (finite) peak. We note that in the case of "perfect nesting" [6] the *bare* susceptibility at zero temperature diverges at the nesting vectors $\mathbf{Q}$, so that any finite coupling g leads to an instability already at some finite critical temperature in RPA.

To analyze the behavior of the susceptibility near the singularity, we expand

$$\delta\Pi_0(\mathbf{q}, \omega) = \Pi_0(\mathbf{q}, \omega) - \Pi_0(\mathbf{Q}, 0), \quad (5)$$

for $\mathbf{q}$ near $\mathbf{Q}$ and small ω. Momenta near $\mathbf{Q}$ are parametrized by relative momentum coordinates q_r and q_t, parallel and perpendicular to $\mathbf{Q}$, respectively. The leading contributions to $\delta\Pi_0(\mathbf{q}, \omega)$ come from fermionic momenta near the hot spots connected by $\mathbf{Q}$, where the dispersion relations in Eq. (4) can be expanded as in Eq. (1), that is, $\xi_\mathbf{k} = v_F k_r + b k_t^4$ and $\xi_{\mathbf{k}-\mathbf{q}} = -v_F(k_r - q_r) + b(k_t - q_t)^4$. In the following we assume that b is positive. Our derivations and results can be easily adapted to negative b. The integrals over k_r, k_t, and k_0 are evaluated in Appendix.

For $q_t = 0$, the integral in Eq. (4) is elementary, yielding

$$\delta\Pi_0(q_r, 0, \omega) = \frac{1}{4\pi v_F (2b)^{1/4}} [(1 - i)\sqrt[4]{\omega + i0^+ - v_F q_r}$$

$$+ (1 + i)\sqrt[4]{-\omega - i0^+ - v_F q_r}]. \quad (6)$$

In the static limit $\omega \to 0$, one obtains

$$\delta\Pi_0(q_r, 0, 0) = \begin{cases} (v_F |q_r|)^{1/4}/[2\pi v_F (2b)^{1/4}] & \text{for } q_r < 0, \\ (v_F q_r)^{1/4}/[\sqrt{2}\pi v_F (2b)^{1/4}] & \text{for } q_r > 0. \end{cases} \quad (7)$$

The static particle-hole bubble thus exhibits a cusp with infinite slope as a function of q_r at $q_r = q_t = 0$. For $q_t \neq 0$, the particle-hole bubble can be expressed in a scaling form as (see
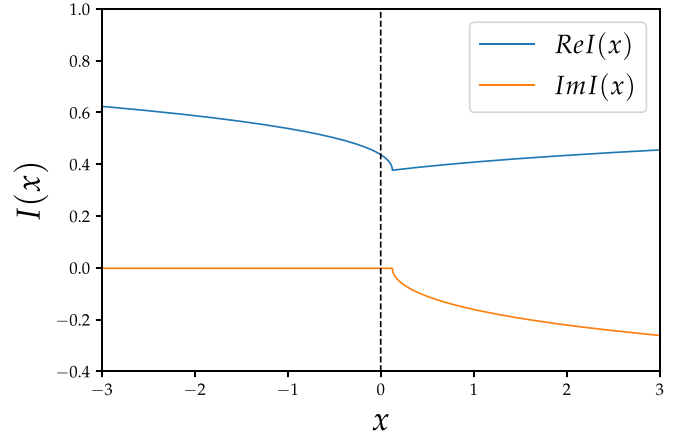

FIG. 3. Real and imaginary parts of the scaling function $I(x)$.

Appendix)

$$\delta\Pi_0(q_r, q_t, \omega) = \frac{|q_t|}{4v_F} \left[I\left(\frac{\omega - v_F q_r}{b q_t^4}\right) + I^*\left(\frac{-\omega - v_F q_r}{b q_t^4}\right) \right], \quad (8)$$

where

$$I(x) = \int_0^\infty \frac{d\tilde{k}_0}{2\pi} \left[\frac{1 + i}{2(i\tilde{k}_0)^{3/4}} \right. $$
$$\left. - \frac{\frac{1}{\sqrt{-\frac{3}{4} + \sqrt{\frac{1}{2}(1 + x + 2i\tilde{k}_0)}}} + \frac{1}{\sqrt{-\frac{3}{4} - \sqrt{\frac{1}{2}(1 + x + 2i\tilde{k}_0)}}}}{\sqrt{2(1 + x + 2i\tilde{k}_0)}} \right] \quad (9)$$

is a dimensionless scaling function, shown graphically in Fig. 3. The graph of $I(x)$ exhibits a cusp at $x = \frac{1}{8}$, and the imaginary part of $I(x)$ vanishes for all $x \leqslant \frac{1}{8}$. While $I(x)$ cannot be expressed by elementary functions, $I(0)$ and $I(\frac{1}{8})$ are given by the simple numbers $\sqrt{2}/\pi$ and $\sqrt{\frac{3}{2}}/\pi$, respectively. Since $I(0)$ is finite, $\delta\Pi_0(0, q_t, 0)$ is linear in $|q_t|$. For $|x| \to \infty$, the scaling function behaves asymptotically as

$$I(x) \sim \begin{cases} \frac{1-i}{2^{1/4}\pi} x^{1/4} & + \frac{3 \cdot 2^{1/4}(1+i)}{8\pi} x^{-1/4} & \text{for } x > 0, \\ \frac{2^{1/4}}{\pi} |x|^{1/4} & + \frac{3}{4 \cdot 2^{1/4}\pi} |x|^{-1/4} & \text{for } x < 0. \end{cases} \quad (10)$$

Inserting the leading asymptotic behavior into Eq. (8) one recovers the result Eq. (6) for $q_t = 0$. The next-to-leading order yields the leading q_t dependence for $b|q_t|^4 \ll |\pm\omega - v_F q_r|$,

$$\Pi_0(q_r, q_t, \omega) - \Pi_0(q_r, 0, \omega)$$

$$= \frac{3(2b)^{1/4} q_t^2}{32\pi v_F} \times \left(\frac{1 + i}{\sqrt[4]{\omega + i0^+ - v_F q_r}} \right. $$
$$\left. + \frac{1 - i}{\sqrt[4]{-\omega - i0^+ - v_F q_r}} \right) + \mathcal{O}(q_t^4), \quad (11)$$

Hence, for $\omega \neq \pm v_F q_r$, the leading q_t dependence is quadratic in q_t.

The RPA effective interaction is given by

$$D(\mathbf{q}, iq_0) = \frac{g}{1 + g\chi_0(\mathbf{q}, iq_0)} \quad (12)$$

on the imaginary frequency axis, and by the same expression with $iq_0 \to \omega$ on the real frequency axis. At the QCP, $g\chi_0(\mathbf{Q}, 0)$ is equal to minus one, so that

$$D(\mathbf{q}, \omega) = -\frac{1}{N\delta\Pi_0(\mathbf{q}, \omega)}. \quad (13)$$

Hence, the effective interaction at the QCP does not depend on the coupling constant g.

III. FERMION SELF-ENERGY

To leading order in the effective interaction D, the fermion self-energy is given by the one-loop integral,

$$\Sigma(\mathbf{k}, ik_0) = -M \int_{\mathbf{q}} \int_{q_0} D(\mathbf{q}, iq_0) G_0(\mathbf{k} - \mathbf{q}, ik_0 - iq_0), \quad (14)$$

with $M = 1$ for a charge-density and $M = 3$ for a spin-density instability [13]. Analytic continuation of this expression to the real frequency axis yields [21]

$$
\begin{aligned}
&\Sigma(\mathbf{k}, \omega + i0^+) \\
&= -\frac{M}{\pi} \int d\nu \int_{\mathbf{q}} \big[b(\nu) \, \mathrm{Im} D(\mathbf{q}, \nu + i0^+) \\
&\quad \times G_0(\mathbf{k} - \mathbf{q}, \nu + \omega + i0^+) \\
&\quad - f(\nu) D(\mathbf{q}, \nu - \omega - i0^+) \, \mathrm{Im} G_0(\mathbf{k} - \mathbf{q}, \nu + i0^+) \big],
\end{aligned}
\quad (15)
$$

where $b(\nu) = [e^{\beta\nu} - 1]^{-1}$ and $f(\nu) = [e^{\beta\nu} + 1]^{-1}$ are the Bose and Fermi functions, respectively. At zero temperature ($\beta = \infty$) these functions become step functions $b(\nu) = -\Theta(-\nu)$ and $f(\nu) = \Theta(-\nu)$. In the following we denote $\Sigma(\mathbf{k}, \omega + i0^+)$, $G(\mathbf{k}, \omega + i0^+)$, and $D(\mathbf{q}, \nu + i0^+)$ by $\Sigma(\mathbf{k}, \omega)$, $G(\mathbf{k}, \omega)$, and $D(\mathbf{q}, \nu)$, respectively. Note, however, the negative infinitesimal imaginary part in one of the frequency arguments in Eq. (15).

We analyze $\Sigma(\mathbf{k}, \omega)$ at the QCP for low frequencies ω and momenta $\mathbf{k}$ near one of the hot spots on the Fermi surface, which we denote as $\mathbf{k}_H$. The effective interaction D at the QCP is given by Eq. (13) with $\delta\Pi_0$ from Eq. (8). The dominant contributions come from momentum transfers $\mathbf{q}$ near $\mathbf{Q}$, so that $\mathbf{k} - \mathbf{q}$ is situated near the antipodal hot spot $-\mathbf{k}_H$. Using relative momentum variables as above, the dispersion relation in the fermion propagator can be expanded as $\xi_{\mathbf{k}-\mathbf{q}} = -v_F(k_r - q_r) + b(k_t - q_t)^4$.

To evaluate the self-energy, it is convenient to first consider its imaginary part, and then compute the real part from a Kramers-Kronig relation. The imaginary part of Eq. (15) reads

$$
\begin{aligned}
\mathrm{Im}\Sigma(\mathbf{k}, \omega) &= -\frac{M}{\pi} \int d\nu \int_{\mathbf{q}} [b(\nu) + f(\nu + \omega)] \, \mathrm{Im} D(\mathbf{q}, \nu) \\
&\quad \times \mathrm{Im} G_0(\mathbf{k} - \mathbf{q}, \omega + \nu).
\end{aligned}
\quad (16)
$$

Note that $\mathrm{Im} D(\mathbf{q}, \nu - i0^+) = -\mathrm{Im} D(\mathbf{q}, \nu + i0^+)$. Using the Dirac identity $\mathrm{Im} G_0(\mathbf{k}, \omega) = -\pi\delta(\omega - \xi_{\mathbf{k}})$, the frequency integral in Eq. (16) can be easily carried out, yielding

$$
\begin{aligned}
\mathrm{Im}\Sigma(\mathbf{k}, \omega) &= M \int_{\mathbf{q}} [b(\xi_{\mathbf{k}-\mathbf{q}} - \omega) + f(\xi_{\mathbf{k}-\mathbf{q}})] \\
&\quad \times \mathrm{Im} D(\mathbf{q}, \xi_{\mathbf{k}-\mathbf{q}} - \omega).
\end{aligned}
\quad (17)
$$

At zero temperature, the sum of Bose and Fermi functions in Eq. (17) is given by

$$b(\xi_{\mathbf{k}-\mathbf{q}} - \omega) + f(\xi_{\mathbf{k}-\mathbf{q}}) = \begin{cases} -1 & \text{for } 0 < \xi_{\mathbf{k}-\mathbf{q}} < \omega, \\ 1 & \text{for } \omega < \xi_{\mathbf{k}-\mathbf{q}} < 0, \\ 0 & \text{else,} \end{cases} \quad (18)$$

restricting thus the contributing momentum region. The integral in Eq. (17) is convergent even if the momentum integration over q_r and q_t is extended to infinity.

The real part of the self-energy can be obtained from the Kramers-Kronig-type relation,

$$\Sigma(\mathbf{k}, \omega) = -\frac{1}{\pi} \int_{-\infty}^{\infty} d\omega' \frac{\mathrm{Im}\Sigma(\mathbf{k}, \omega')}{\omega - \omega' + i0^+} + \text{const}. \quad (19)$$

The last term in this relation is a real constant.

A. Frequency dependence at hot spot

The frequency dependence at the hot spot (for $\mathbf{k} = \mathbf{k}_H$) can be derived by a simple rescaling of the integration variables in Eq. (17). Substituting $q_r = |\omega/v_F| \tilde{q}_r$ and $q_t = |\omega/b|^{1/4} \tilde{q}_t$, one obtains

$$\mathrm{Im}\Sigma(\mathbf{k}_H, \omega) = -\frac{M}{N} A_{s(\omega)} |\omega|, \quad (20)$$

where A_+ and A_- are two positive dimensionless numbers depending on the sign of ω. These numbers are determined by the integral,

$$A_{s(\omega)} = -\int_{\tilde{\mathbf{q}}}' \mathrm{Im} \frac{4s(\omega)}{|\tilde{q}_t| \left[I\left(\frac{\tilde{q}_t^4 - s(\omega)}{\tilde{q}_t^4}\right) + I^*\left(\frac{-2\tilde{q}_r - \tilde{q}_t^4 + s(\omega)}{\tilde{q}_t^4}\right) \right]}, \quad (21)$$

where the prime at the integral sign indicates a restriction of the integration region to $0 < \tilde{q}_r + \tilde{q}_t^4 < 1$ for $\omega > 0$, and to $-1 < \tilde{q}_r + \tilde{q}_t^4 < 0$ for $\omega < 0$. Note that the frequency dependence of the self-energy at the hot spot depends neither on v_F, nor on b. A numerical evaluation of the integral in Eq. (21) yields $A_+ \approx 0.049$ and $A_- \approx 0.072$. Hence, $\mathrm{Im}\Sigma(\mathbf{k}_H, \omega)$ is slightly asymmetric in ω. For the generic situation with a finite Fermi surface curvature, a linear frequency dependence of $\mathrm{Im}\Sigma(\mathbf{k}_H, \omega)$ with asymmetric coefficients has also been found in a one-loop calculation of the self-energy at the onset of charge- or spin-density wave order with *two* pairs of nested hot spots connected by the same wave vector $\mathbf{Q}$ [12,14]. In that case, however, the coefficients are not universal—they depend on a dimensionless combination of model parameters.

The real part of the self-energy can be obtained from the Kramers-Kronig relation Eq. (19). With $\mathrm{Im}\Sigma(\mathbf{k}_H, \omega)$ as in Eq. (20), the integral in Eq. (19) is logarithmically divergent at large frequencies ω'. This is due to the fact that the linear frequency dependence has been obtained from an expansion that captures only the asymptotic low-frequency behavior, which cannot be extended to all frequencies. The imaginary part of the exact self-energy of any physical system has to vanish in the high-frequency limit. To compute the low-frequency behavior of $\mathrm{Re}\Sigma$, we mimic the high-frequency decay of $\mathrm{Im}\Sigma$ by imposing an ultraviolet frequency cutoff Λ_ω, so that the frequency integration in Eq. (19) is restricted to $|\omega'| < \Lambda_\omega$. Defining $\delta\Sigma(\mathbf{k}, \omega) = \Sigma(\mathbf{k}, \omega) - \Sigma(\mathbf{k}_H, 0)$, we then obtain

$$\mathrm{Re}\,\delta\Sigma(\mathbf{k}_H, \omega) = -\frac{M}{N} \frac{A_+ + A_-}{\pi} \omega \ln \frac{\Lambda_\omega}{|\omega|}, \quad (22)$$

for $|\omega| \ll \Lambda_\omega$.

The logarithm in Eq. (22) implies a logarithmic divergence of the inverse quasiparticle weight [19], $Z^{-1} = 1 - \partial \Sigma(\mathbf{k}_H, \omega)/\partial \omega \sim \ln(\Lambda_\omega/|\omega|)$. Hence, Landau quasiparticles do not exist at the hot spots, and Fermi liquid theory breaks down.

Logarithmic divergencies are frequently a perturbative manifestation of power-law behavior, especially in (quantum) critical systems. Assuming that the one-loop result in Eq. (22) reflects the leading order of an expansion of a power law, one obtains

$$\omega - \delta \Sigma(\mathbf{k}_H, \omega) \propto (|\omega|/\Lambda_\omega)^{-\eta_\omega} \omega \qquad (23)$$

at low frequencies, with the anomalous dimension,

$$\eta_\omega = \frac{M}{N} \frac{A_+ + A_-}{\pi} \approx \frac{M}{N} 0.039. \qquad (24)$$

Hence, the quasiparticle weight Z vanishes as $|\omega|^{\eta_\omega}$ in the low-energy limit. Note that Kramers-Kronig consistency requires that the real and imaginary parts of the self-energy obey the same power law if $\eta_\omega > 0$. We emphasize that the power law in Eq. (23) is only an educated guess. The actual behavior might be more complicated. To clarify the role of higher order contributions, a renormalization group analysis might be a useful next step.

B. Frequency and momentum dependencies near hot spot

We now analyze the momentum and frequency dependence of the self-energy in the vicinity of a hot spot. We consider radial and tangential momentum dependencies separately. For $k_t = 0$, we can express $\text{Im} \Sigma(\mathbf{k}, \omega)$ from Eq. (17) in the scaling form,

$$\text{Im} \Sigma(\mathbf{k}, \omega) = -\frac{M}{N} A^{(r)}_{s(\omega)}(\tilde{k}_r) |\omega|, \qquad (25)$$

with the dimensionless scaling functions

$$A^{(r)}_{s(\omega)}(\tilde{k}_r)$$
$$= -\int'_{\tilde{\mathbf{q}}} \text{Im} \frac{4s(\omega)}{|\tilde{q}_t| \left[I \left(\frac{-\tilde{k}_r + \tilde{q}_t^4 - s(\omega)}{\tilde{q}_t^2} \right) + I^* \left(\frac{\tilde{k}_r - 2\tilde{q}_r - \tilde{q}_t^4 + s(\omega)}{\tilde{q}_t^2} \right) \right]}, \qquad (26)$$

where the integration region is restricted to $0 < -\tilde{k}_r + \tilde{q}_r + \tilde{q}_t^4 < 1$ for $\omega > 0$, and to $-1 < -\tilde{k}_r + \tilde{q}_r + \tilde{q}_t^4 < 0$ for $\omega < 0$. The rescaled variables are defined by $q_r = |\omega/v_F|\tilde{q}_r$, $q_t = |\omega/b|^{1/4}\tilde{q}_t$, and $k_r = |\omega/v_F|\tilde{k}_r$. The scaling functions $A^{(r)}_\pm$ are shown graphically in Fig. 4. For $\tilde{k}_r = 0$ we recover Eq. (20), since $A^{(r)}_\pm(0) = A_\pm$ from Eq. (21). For small finite $\tilde{k}_r$, the leading $\tilde{k}_r$ dependence of $A^{(r)}_{s(\omega)}(\tilde{k}_r)$ is linear,

$$A^{(r)}_\pm(\tilde{k}_r) = A_\pm + B_\pm \tilde{k}_r + \mathcal{O}(\tilde{k}_r^2), \qquad (27)$$

with $B_+ \approx -0.050$ and $B_- \approx 0.027$. In Fig. 5 we show the frequency dependence of $\text{Im} \Sigma(\mathbf{k}, \omega)$ for various choices of k_r. For small $|\omega|$, the leading frequency dependence is quadratic. For $|\omega| \gg v_F |k_r|$, the curves rapidly approach the asymptotic behavior,

$$\text{Im} \Sigma(\mathbf{k}, \omega) \sim -\frac{M}{N} [A_{s(\omega)} |\omega| + B_{s(\omega)} v_F k_r], \qquad (28)$$
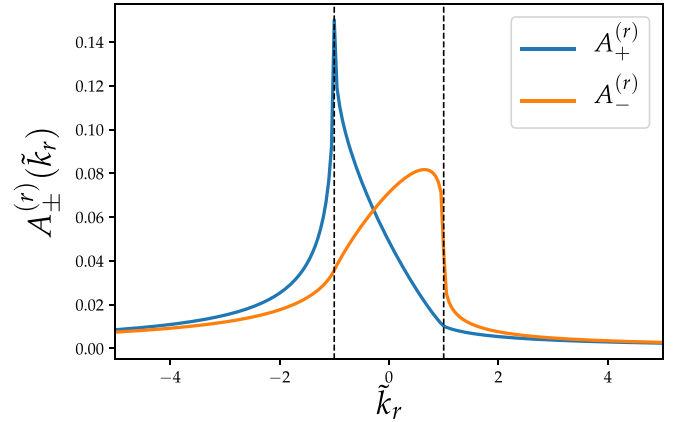

FIG. 4. Scaling functions $A^{(r)}_\pm(\tilde{k}_r)$. The vertical dashed lines mark the location of singularities at $\tilde{k}_r = \pm 1$.

which follows from Eq. (27). Inserting this asymptotic dependence in the Kramers-Kronig relation Eq. (19), one obtains the leading k_r dependence of the real part of the self-energy at zero frequency as

$$\delta \Sigma(\mathbf{k}, 0) \sim -\frac{M}{N} \frac{B_+ - B_-}{\pi} v_F k_r \ln \frac{\Lambda_\omega}{v_F |k_r|}. \qquad (29)$$

Assuming, as before, that the logarithm reflects the leading contribution from a power law, we expect a momentum dependence of the form,

$$v_F k_r + \delta \Sigma(\mathbf{k}, 0) \propto (v_F |k_r|/\Lambda_\omega)^{-\eta_r} v_F k_r, \qquad (30)$$

for small k_r, with the anomalous dimension,

$$\eta_r = \frac{M}{N} \frac{B_- - B_+}{\pi} \approx \frac{M}{N} 0.025. \qquad (31)$$

The renormalized Fermi velocity [19] given by $\bar{v}_F(k_r) = Z[1 + \partial \Sigma/\partial k_r] v_F$ is proportional to $|\omega|^{\eta_\omega} |k_r|^{-\eta_r}$ with $\omega = v_F k_r$, and thus $\bar{v}_F(k_r) \propto |k_r|^{\eta_\omega - \eta_r}$. This quantity vanishes for $k_r \to 0$, albeit very slowly, since $\eta_\omega > \eta_r$. We now discuss the tangential momentum dependence of the self-energy. For $k_r = 0$, we can express $\text{Im} \Sigma(\mathbf{k}, \omega)$ from Eq. (17) in the scaling
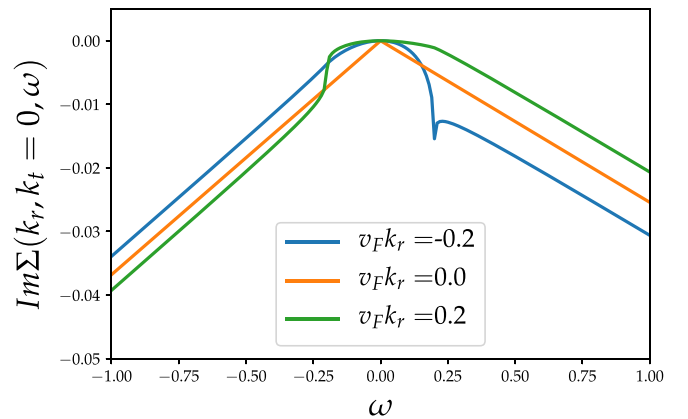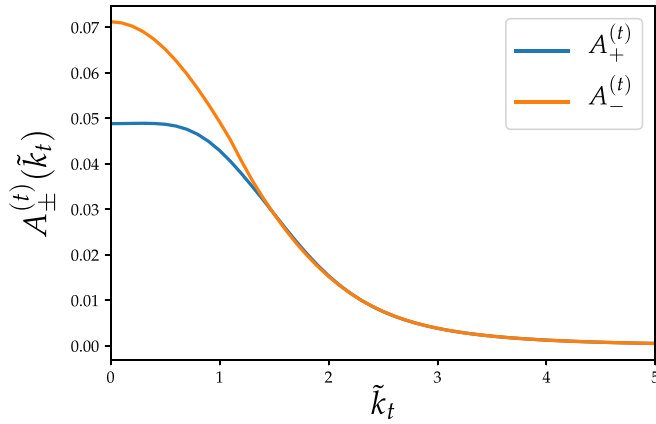

FIG. 5. Imaginary part of the one-loop self-energy as a function of frequency for various choices of the radial momentum variable k_r. Here $M = 1$ and $N = 2$.

FIG. 6. Scaling functions $A_{\pm}^{(t)}(\tilde{k}_t)$.

FIG. 7. Imaginary part of the one-loop self-energy as a function of frequency for various choices of the tangential momentum variable k_t. Here $M = 1$ and $N = 2$.

form,

$$\text{Im}\Sigma(\mathbf{k}, \omega) = -\frac{M}{N} A_{s(\omega)}^{(t)}(\tilde{k}_t) |\omega|, \quad (32)$$

with the dimensionless scaling functions (see also Fig. 6),

$$
A_{s(\omega)}^{(t)}(\tilde{k}_t)
$$
$$
= -\int_{\tilde{\mathbf{q}}}' \text{Im} \frac{4s(\omega)}{|\tilde{q}_t|\left[I\left(\frac{(\tilde{k}_t - \tilde{q}_t)^4 - s(\omega)}{\tilde{q}_t^4}\right) + I^*\left(\frac{-2\tilde{q}_r - (\tilde{k}_t - \tilde{q}_t)^4 + s(\omega)}{\tilde{q}_t^4}\right)\right]}, \quad (33)
$$

where the integration region is restricted to $0 < \tilde{q}_r + (\tilde{k}_t - \tilde{q}_t)^4 < 1$ for $\omega > 0$, and to $-1 < \tilde{q}_r + (\tilde{k}_t - \tilde{q}_t)^4 < 0$ for $\omega < 0$. The rescaled variables are defined by $q_r = |\omega/v_F|\tilde{q}_r$, $q_t = |\omega/b|^{1/4}\tilde{q}_t$, and $k_t = |\omega/b|^{1/4}\tilde{k}_t$. The scaling functions $A_{\pm}^{(t)}(\tilde{k}_t)$ are symmetric under $\tilde{k}_t \mapsto -\tilde{k}_t$. Hence, their Taylor expansion for small $\tilde{k}_t$ contains only even powers of $\tilde{k}_t$,

$$A_{\pm}^{(t)}(\tilde{k}_t) = A_{\pm} + C_{\pm}\tilde{k}_t^2 + D_{\pm}\tilde{k}_t^4 + \mathcal{O}(\tilde{k}_t^6). \quad (34)$$
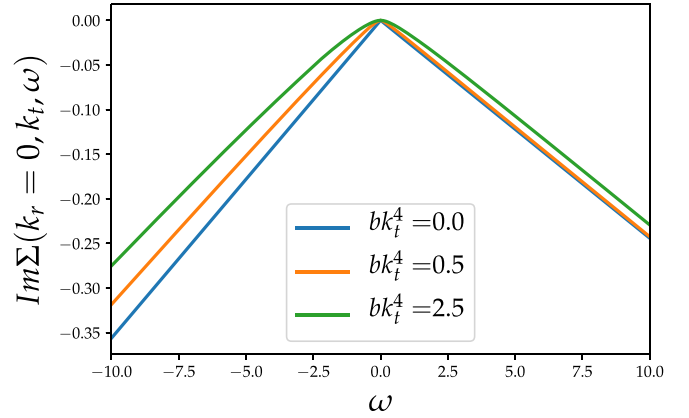
A numerical evaluation of Eq. (33) yields $C_+ = 0$, $C_- \approx -0.023$, $D_+ \approx -0.008$, and $D_- \approx 0.005$. The quartic coefficient D_- is less accurate than the others, because the quartic contribution is superseded by the much larger (for small $\tilde{k}_t$) quadratic term. In Fig. 7 we show the frequency dependence of $\text{Im}\Sigma(\mathbf{k}, \omega)$ for various choices of k_t. For small $|\omega|$, the leading frequency dependence is quadratic. For $|\omega| \gg b|k_t|^4$, the curves approach the asymptotic behavior,

$$\text{Im}\Sigma(\mathbf{k}, \omega) \sim -\frac{M}{N}\left[A_{s(\omega)}|\omega| + C_{s(\omega)}\sqrt{b|\omega|}k_t^2 + D_{s(\omega)}bk_t^4\right]. \quad (35)$$

Inserting this expansion into the Kramers-Kronig relation Eq. (19), we obtain

$$
\delta\Sigma(\mathbf{k}, 0) = -\frac{2M}{\pi N}(C_+ - C_-)\sqrt{b\Lambda_\omega}\,k_t^2
$$
$$
- \frac{M}{\pi N}(D_+ - D_-)bk_t^4 \ln\frac{\Lambda_\omega}{bk_t^4} + \mathcal{O}(k_t^4), \quad (36)
$$

for small k_t. The leading term is quadratic in k_t and depends strongly on the ultraviolet cutoff Λ_ω. This term, along with generic regular many-body contributions of the same order, leads to a renormalized dispersion relation $\bar{\xi}_{\mathbf{k}}$ with a quadratic

tangential momentum dependence, in conflict with our original assumption. However, the case of a dispersion with a vanishing quadratic dependence on k_t can be restored by slightly shifting the bare parameters of our system such that the self-energy corrections cancel the quadratic k_t dependence of the bare dispersion relation. Between parameter regimes with a locally convex and a locally concave Fermi surface (at the hot spots), there must be a transition point where the Fermi surface is flat, in the interacting system as well as in the noninteracting reference model. Hence, we are left with the second term in Eq. (36) only, which can be promoted to a power law of the form,

$$bk_t^4 + \delta\Sigma(\mathbf{k}, 0) \propto \left(bk_t^4/\Lambda_\omega\right)^{-\eta_t} bk_t^4, \quad (37)$$

for small k_t, with the anomalous dimension,

$$\eta_t = \frac{M}{N}\frac{D_- - D_+}{\pi} \approx \frac{M}{N}0.004. \quad (38)$$

Combining the results on the frequency dependence of the quasiparticle weight Z with the results on the radial and tangential momentum dependence of the self-energy, we obtain a renormalized dispersion relation of the form,

$$\bar{\xi}_{\mathbf{k}} = a_r \,\text{sgn}(k_r)|k_r|^{\alpha_r} + a_t|k_t|^{\alpha_t}, \quad (39)$$

where $\alpha_r = 1 + \eta_\omega - \eta_r$ and $\alpha_t = 4(1 + \eta_\omega - \eta_t)$, while a_r and a_t are nonuniversal coefficients. The anomalous dimensions are relatively small, so that α_r and α_t remain close to the bare values one and four, respectively. A renormalized dispersion of the form Eq. (39) has been obtained earlier in an ϵ expansion [15] for the standard case of a bare dispersion with a quadratic tangential momentum dependence. In that case, the anomalous dimensions turned out to be quite large in the physical dimension two (corresponding to $\epsilon = \frac{1}{2}$), leading to a strongly flattened Fermi surface with an almost quartic shape $k_r \propto |k_t|^{3.85}$.

We finally note that one-loop vertex corrections are regular and therefore do not affect the above power laws. For ordering wave vectors distinct from half a reciprocal lattice vector, there is no choice of momenta in the vertex correction at which all the propagators are singular, so that the vertex correction is finite [7].

IV. CONCLUSION

We have analyzed quantum fluctuation effects at the onset of charge- or spin-density wave order with an incommensurate nesting ($2k_F$) wave vector $\mathbf{Q}$ in two-dimensional metals, for the special case where $\mathbf{Q}$ connects a pair of hot spots situated at flat high symmetry points of the Fermi surface with a vanishing Fermi surface curvature. The leading tangential momentum dependence of the bare dispersion is quartic at these points. The charge or spin susceptibilities form a pronounced peak at $\mathbf{Q}$.

We have computed the fermion self-energy $\Sigma(\mathbf{k}, \omega)$ at the QCP as a function of (real) frequency and momentum near the hot spots in RPA, that is, in one-loop approximation. At the hot spots, the frequency dependence of ImΣ is linear and slightly asymmetric, while the quasiparticle weight and the momentum dependence of the self-energy exhibit logarithmic divergencies with universal prefactors. Hence, there are no Landau quasiparticles at the hot spots, giving rise to non-Fermi liquid behavior.

A tentative resummation of the logarithms leads to power laws with small universal anomalous dimensions. The quasiparticle weight vanishes with a small power of frequency. The renormalized dispersion relation has the form $\bar{\xi}_{\mathbf{k}} = a_r \, \mathrm{sgn}(k_r)|k_r|^{\alpha_r} + a_t |k_t|^{\alpha_t}$ near the hot spots, where k_r and k_t are radial and tangential relative momentum variables, respectively. The exponents α_r and α_t are close to the corresponding exponents of the bare dispersion relation one and four, respectively. Since the renormalized dispersion relation has almost the same form as the bare one, and the quasiparticle weight vanishes only slowly, the self-energy corrections do not destroy the peak at the nesting vector in the susceptibility. The $2k_F$ QCP is thus stable. In particular, there are no indications that it might be replaced by a first-order transition, in contrast to the more delicate situation for a quadratic dispersion [7,13].

The QCP with flat hot spots could be realized experimentally in suitable layered compounds or cold atom systems by fine tuning two parameters, for example, density and interaction strength. In solids, the self-energy is directly related to the spectral function for single-electron excitations, which can be measured by angular resolved photoemission spectroscopy. While the renormalization of the dispersion is probably too small to be resolved in experiment, the frequency dependence of the self-energy leads to a sizable broadening of the spectral function and a suppression of spectral weight at low energies, which should be observable. Moreover, our model is an instructive prototype of a larger class of systems with a *bare* dispersion of the form $\xi_{\mathbf{k}} = a_r \, \mathrm{sgn}(k_r)|k_r|^{\alpha_r^{(0)}} + a_t |k_t|^{\alpha_t^{(0)}}$. In our case, where $\alpha_r^{(0)} = 1$ and $\alpha_t^{(0)} = 4$, the analysis is comparatively simple, since several integrations can be performed analytically, and the renormalized dispersion remains close to the bare one. From a theoretical point of view it would be interesting to extend the analysis to more general bare exponents $\alpha_r^{(0)}$ and $\alpha_t^{(0)}$, and see whether the renormalized dispersion has universal exponents. In particular, it remains to be clarified whether in the conventional but delicate case $\alpha_r^{(0)} = 1$ and $\alpha_t^{(0)} = 2$ the mean-field QCP survives in the presence of fluctuations, with a renormalized dispersion of the above form and a flattened Fermi surface, as suggested by the one-loop ϵ expansion by Halbinger *et al.* [15].

ACKNOWLEDGMENTS

APPENDIX: EVALUATION OF PARTICLE-HOLE BUBBLE

The k_r integral in Eq. (4) can be easily carried out by using the residue theorem. Shifting the remaining integration variables as $k_t \to k_t + q_t/2$ and $k_0 \to k_0 + q_0/2$ to symmetrize the integrand, one obtains

$$\Pi_0(\mathbf{q}, iq_0)$$
$$= \frac{i}{v_F} \int_{-\infty}^{\infty} \frac{dk_0}{2\pi} \int_{-\infty}^{\infty} \frac{dk_t}{2\pi}$$
$$\times \frac{\Theta(-k_0 - q_0/2) - \Theta(k_0 - q_0/2)}{2ik_0 - v_F q_r - b(k_t + q_t/2)^4 - b(k_t - q_t/2)^4}. \quad \text{(A1)}$$

The k_t integration can also be performed via residues. The denominator in Eq. (A1) has four poles in the complex k_t plane, namely

$$k_t^{ss'} = s\sqrt{-\frac{3}{4}q_t^2 + \frac{s'}{\sqrt{2}}\sqrt{q_t^4 + (2ik_0 - v_F q_r)/b}}, \quad \text{(A2)}$$

where $s, s' \in \{+, -\}$. Closing the integration contour in the upper complex half-plane, only the poles in the upper half-plane contribute. For $k_0 > 0$, these are the poles k_t^{++} and k_t^{--}, and the corresponding residues are

$$R^{++} = \frac{1}{(k_t^{++} - k_t^{+-})(k_t^{++} - k_t^{-+})(k_t^{++} - k_t^{--})}$$
$$= \frac{1}{2\sqrt{2}k_t^{++}\sqrt{q_t^4 + (2ik_0 - v_F q_r)/b}}, \quad \text{(A3a)}$$

$$R^{--} = \frac{1}{(k_t^{--} - k_t^{++})(k_t^{--} - k_t^{+-})(k_t^{--} - k_t^{-+})}$$
$$= \frac{-1}{2\sqrt{2}k_t^{--}\sqrt{q_t^4 + (2ik_0 - v_F q_r)/b}}. \quad \text{(A3b)}$$

For $k_0 < 0$, the poles k_t^{+-} and k_t^{-+} are situated in the upper half-plane, and the corresponding residues are

$$R^{+-} = \frac{1}{(k_t^{+-} - k_t^{++})(k_t^{+-} - k_t^{-+})(k_t^{+-} - k_t^{--})}$$
$$= -R^{--}, \quad \text{(A4a)}$$

$$R^{-+} = \frac{1}{(k_t^{-+} - k_t^{++})(k_t^{-+} - k_t^{+-})(k_t^{-+} - k_t^{--})}$$
$$= -R^{++}, \quad \text{(A4b)}$$

where R^{++} and R^{--} are defined by the expressions on the right-hand sides of Eq. (A3), but now for $k_0 < 0$. The numerator in Eq. (A1) partitions the k_0 axis in three regions,

$$\Theta(-k_0 - q_0/2) - \Theta(k_0 - q_0/2)$$
$$= \begin{cases} 1 & \text{for} \quad k_0 < -|q_0|/2 \\ 0 & \text{for} \quad -|q_0|/2 < k_0 < |q_0|/2 \,. \\ -1 & \text{for} \quad k_0 > |q_0|/2 \end{cases} \quad \text{(A5)}$$

Performing the k_t integral in Eq. (A1) by using the residue theorem, one thus obtains

$$\Pi_0(\mathbf{q}, iq_0) = -\frac{1}{2bv_F} \int_{-\infty}^{\infty} \frac{dk_0}{2\pi} \Theta(|k_0| - |q_0|/2)(R^{++} + R^{--}).$$

(A6)

The integral diverges in the ultraviolet, but the integral for $\delta\Pi_0(\mathbf{q}, iq_0) = \Pi_0(\mathbf{q}, iq_0) - \Pi_0(\mathbf{Q}, 0)$ is finite.

In the special case $q_t = 0$, the k_0 integral in Eq. (A6) is elementary. Setting $q_t = 0$, one obtains

$$k_t^{++}(q_t = 0) = \left(\frac{2ik_0 - v_F q_r}{2b}\right)^{1/4},$$

(A7a)

$$k_t^{--}(q_t = 0) = \left(\frac{2ik_0 - v_F q_r}{2b}\right)^{1/4} is(k_0),$$

(A7b)

where $s(k_0)$ is the sign of k_0. The residues simplify to

$$R^{++}(q_t = 0) = \frac{1}{4}\left(\frac{2ik_0 - v_F q_r}{2b}\right)^{-3/4},$$

(A8a)

$$R^{--}(q_t = 0) = \frac{i}{4}\left(\frac{2ik_0 - v_F q_r}{2b}\right)^{-3/4} s(k_0).$$

(A8b)

Inserting this into Eq. (A6) and introducing an ultraviolet cutoff Λ, we obtain

$$\Pi_0(q_r, 0, iq_0) = -\frac{1}{8bv_F} \int_{-\Lambda}^{\Lambda} \frac{dk_0}{2\pi} \Theta(|k_0| - |q_0|/2)$$
$$\times \left(\frac{2ik_0 - v_F q_r}{2b}\right)^{-3/4} [1 + s(k_0)]. \quad \text{(A9)}$$

The frequency integration is obviously elementary. Subtracting $\Pi_0(0, 0, 0)$, we can take the limit $\Lambda \to \infty$, yielding

$$\delta\Pi_0(q_r, 0, iq_0) = \frac{1}{4\pi v_F(2b)^{1/4}}[(1 - i)\sqrt[4]{i|q_0| - v_F q_r}$$
$$+ (1 + i)\sqrt[4]{-i|q_0| - v_F q_r}\,]. \quad \text{(A10)}$$

Analytic continuation of this expression in the upper complex frequency half-plane to real frequencies yields Eq. (6).

For $q_t \neq 0$ we write Π_0 as a sum of two terms, $\Pi_0 = \Pi_0^+ + \Pi_0^-$, where Π_0^+ and Π_0^- are obtained from the contributions with $k_0 > 0$ and $k_0 < 0$ to the integral in Eq. (A6), respectively. Shifting the integration variable by $\pm|q_0|/2$, one obtains

$$\Pi_0^-(\mathbf{q}, iq_0) = -\frac{1}{4bv_F} \int_{-\infty}^{0} \frac{dk_0}{2\pi} \frac{1}{\sqrt{2}\sqrt{q_t^4 + \frac{2ik_0 - i|q_0| - v_F q_r}{b}}}$$
$$\times \sum_{s=\pm 1} \frac{1}{\sqrt{-\frac{3}{4}q_t^2 + \frac{s}{\sqrt{2}}\sqrt{q_t^4 + \frac{2ik_0 - i|q_0| - v_F q_r}{b}}}},$$

$$\Pi_0^+(\mathbf{q}, iq_0) = -\frac{1}{4bv_F} \int_{0}^{\infty} \frac{dk_0}{2\pi} \frac{1}{\sqrt{2}\sqrt{q_t^4 + \frac{2ik_0 + i|q_0| - v_F q_r}{b}}}$$
$$\times \sum_{s=\pm 1} \frac{1}{\sqrt{-\frac{3}{4}q_t^2 + \frac{s}{\sqrt{2}}\sqrt{q_t^4 + \frac{2ik_0 + i|q_0| - v_F q_r}{b}}}}.$$

(A11)

The integrals in Eq. (A11) are UV divergent. Subtracting $\Pi_0^\pm(\mathbf{Q}, 0)$, one obtains finite expressions for $\delta\Pi_0^\pm(\mathbf{q}, iq_0) = \Pi_0^\pm(\mathbf{q}, iq_0) - \Pi_0^\pm(\mathbf{Q}, 0)$.

Equation (A11) can be continued analytically to the entire upper complex frequency half-plane by simply extending $i|q_0| \to z$ with $\text{Im}\, z > 0$ (note that $|q_0| = q_0$ in the upper frequency plane). One can easily check that the integrands encounter no poles or branch cuts for $\text{Im}\, z > 0$, for any k_0. Hence, the continuation to real frequencies is obtained by substituting $i|q_0| \to \omega + i0^+$. Moreover, since k_0 and q_0 enter via the linear combinations $2ik_0 - i|q_0|$ for $k_0 < 0$ and $2ik_0 + i|q_0|$ for $k_0 > 0$, the infinitesimal imaginary part $i0^+$ is redundant and can be dropped. At this point it is clear that $\delta\Pi_0^-$ and $\delta\Pi_0^+$ depend on q_r and ω only via the linear combinations $-\omega - v_F q_r$ and $\omega - v_F q_r$, respectively. Substituting k_0 by $-k_0$ in the integral for Π_0^-, the analytic continuation of Eq. (A11) to real frequencies can be written as

$$\Pi_0^\pm(\mathbf{q}, \omega) = -\frac{1}{4bv_F} \int_{0}^{\infty} \frac{dk_0}{2\pi} \frac{1}{\sqrt{2}\sqrt{q_t^4 + \frac{\pm 2ik_0 \pm \omega - v_F q_r}{b}}}$$
$$\times \sum_{s=\pm 1} \frac{1}{\sqrt{-\frac{3}{4}q_t^2 + \frac{s}{\sqrt{2}}\sqrt{q_t^4 + \frac{\pm 2ik_0 \pm \omega - v_F q_r}{b}}}}.$$

(A12)

To obtain the scaling form Eq. (8), we introduce a dimensionless integration variable $\tilde{k}_0$ defined by $k_0 = b|q_t|^4\tilde{k}_0$, yielding

$$\Pi_0^\pm(\mathbf{q}, \omega) = -\frac{|q_t|}{4bv_F} \int_{0}^{\infty} \frac{d\tilde{k}_0}{2\pi} \frac{1}{\sqrt{2}\sqrt{1 \pm 2i\tilde{k}_0 + \frac{\pm\omega - v_F q_r}{bq_t^4}}}$$
$$\times \sum_{s=\pm 1} \frac{1}{\sqrt{-\frac{3}{4} + \frac{s}{\sqrt{2}}\sqrt{1 \pm 2i\tilde{k}_0 + \frac{\pm\omega - v_F q_r}{bq_t^4}}}}.$$

(A13)

Subtracting $\Pi_0^\pm(\mathbf{Q}, 0)$ with the same substitution we obtain

$$\delta\Pi_0^\pm(\mathbf{q}, \omega) = \frac{|q_t|}{4v_F} I^\pm\left(\frac{\pm\omega - v_F q_r}{bq_t^4}\right),$$

(A14)

with the dimensionless scaling functions,

$$I^\pm(x) = \int_{0}^{\infty} \frac{d\tilde{k}_0}{2\pi}\left[\frac{1 \pm i}{2(\pm i\tilde{k}_0)^{3/4}}\right.$$
$$\left. - \frac{\frac{1}{\sqrt{-\frac{3}{4} + \sqrt{\frac{1}{2}(1 + x \pm 2i\tilde{k}_0)}}} + \frac{1}{\sqrt{-\frac{3}{4} - \sqrt{\frac{1}{2}(1 + x \pm 2i\tilde{k}_0)}}}}{\sqrt{2(1 + x \pm 2i\tilde{k}_0)}}\right].$$

(A15)

Obviously $I^+(x)$ and $I^-(x)$ are related by complex conjugation, that is, $I^+(x) = [I^-(x)]^*$. Denoting $I^+(x)$ as $I(x)$, we obtain Eqs. (8) and (9).

[1] H. v. Löhneysen, A. Rosch, M. Vojta, and P. Wölfle, Fermi liquid instabilities at magnetic quantum phase transitions, Rev. Mod. Phys. **79**, 1015 (2007).

[2] A. Abanov, A. V. Chubukov, and J. Schmalian, Quantum critical theory of the spin-fermion model and its applications to cuprates: Normal state analysis, Adv. Phys. **52**, 119 (2003).

[3] M. A. Metlitski and S. Sachdev, Quantum phase transitions of metals in two spatial dimensions. II. Spin density wave order, Phys. Rev. B **82**, 075128 (2010).

[4] S.-S. Lee, Recent developments in non-Fermi liquid theory, Annu. Rev. Condens. Matter Phys. **9**, 227 (2018).

[5] E. Berg, M. A. Metlitski, and S. Sachdev, Sign-problem-free quantum Monte Carlo at the onset of antiferromagnetism in metals, Science **338**, 1606 (2012).

[6] This notion of nesting must not be confused with the stronger condition of *perfect nesting*, where a momentum shift **Q** maps extended Fermi surface pieces on top of each other. Perfect nesting occurs only for special band structures and electron densities.

[7] B. L. Altshuler, L. B. Ioffe, and A. J. Millis, Critical behavior of the $T = 0$ $2k_F$ density-wave phase transition in a two-dimensional Fermi liquid, Phys. Rev. B **52**, 5563 (1995).

[8] D. Bergeron, D. Chowdhury, M. Punk, S. Sachdev, and A.-M. S. Tremblay, Breakdown of Fermi liquid behavior at the $(\pi, \pi) = 2k_F$ spin-density wave quantum critical point: The case of electron-doped cuprates, Phys. Rev. B **86**, 155123 (2012).

[9] Y. Wang and A. Chubukov, Quantum-critical pairing in electron-doped cuprates, Phys. Rev. B **88**, 024516 (2013).

[10] In conventional Fermi liquids the quasiparticle decay rate is a quadratic function of the excitation energy in the low-energy limit (with a logarithmic correction in two dimensions). In Refs. [8,9] a smaller exponent $\frac{3}{2}$ is found, instead of two, which one may view as a breakdown of Fermi liquid behavior, as suggested by the title of Ref. [8]. On the other hand, Landau quasiparticles are still well defined in the low-energy limit in this case, so that many results from Fermi liquid theory remain valid.

[11] Commensurate wave vectors can be written as a linear combination of reciprocal lattice vectors with rational coefficients, while incommensurate wave vectors cannot. Obviously there are infinitely many possible rational coefficients, but the quantitative effects of commensurability decrease rapidly with the size of their denominators. In a one-loop calculation there is no difference between commensurate and incommensurate cases, as long as 2**Q** is not a reciprocal lattice vector.

[12] T. Holder and W. Metzner, Non-Fermi-liquid behavior at the onset of incommensurate $2k_F$ charge- or spin-density wave order in two dimensions, Phys. Rev. B **90**, 161106(R) (2014).

[13] J. Sýkora, T. Holder, and W. Metzner, Fluctuation effects at the onset of the $2k_F$ density wave order with one pair of hot spots in two-dimensional metals, Phys. Rev. B **97**, 155159 (2018).

[14] J. Sýkora and W. Metzner, Fluctuation effects at the onset of $2k_F$ density wave order with two pairs of hot spots in two-dimensional metals, Phys. Rev. B **104**, 125123 (2021).

[15] J. Halbinger, D. Pimenov, and M. Punk, Incommensurate $2k_F$ density wave quantum criticality in two-dimensional metals, Phys. Rev. B **99**, 195102 (2019).

[16] T. Schäfer, A. A. Katanin, K. Held, and A. Toschi, Interplay of Correlations and Kohn Anomalies in Three Dimensions: Quantum Criticality with a Twist, Phys. Rev. Lett. **119**, 046402 (2017).

[17] C. Gross and I. Bloch, Quantum simulations with ultracold atoms in optical lattices, Science **357**, 995 (2017).

[18] W. Hofstetter and T. Qin, Quantum simulation of strongly correlated condensed matter systems, J. Phys. B: At. Mol. Opt. Phys. **51**, 082001 (2018).

[19] J. W. Negele and H. Orland, *Quantum Many-Particle Systems* (Addison-Wesley, Reading, 1987).

[20] The data for $\chi_0(\mathbf{q}, 0)$ have been provided by Pietro Bonetti.

[21] For a derivation in the analogous case of an RPA in the particle-particle channel see, for example, D. Rohe and W. Metzner, Pair-fluctuation-induced pseudogap in the normal phase of the two-dimensional attractive Hubbard model at weak coupling, Phys. Rev. B **63**, 224509 (2001).